ResearchGate

See discussions, stats, and author profiles for this publication at: https://www.researchgate.net/publication/316533430

2017 One-Year Seismic-Hazard Forecast for the Central and Eastern United States from Induced and Natural Earthquakes

Article *in* Seismological Research Letters · May 2017

DOI: 10.1785/0220170005

CITATIONS
72

READS
183

13 authors, including:

Mark D. Petersen
United States Geological Survey

115 PUBLICATIONS **3,085** CITATIONS

SEE PROFILE

Morgan P. Moschetti
United States Geological Survey

66 PUBLICATIONS **3,237** CITATIONS

SEE PROFILE

Daniel Mcnamara
United States Geological Survey

90 PUBLICATIONS **2,757** CITATIONS

SEE PROFILE

Justin Rubinstein
United States Geological Survey

72 PUBLICATIONS **2,694** CITATIONS

SEE PROFILE

Some of the authors of this publication are also working on these related projects:

Project SCEC UCERF3 View project

Project NSHM 2014 update View project

All content following this page was uploaded by Morgan P. Moschetti on 19 December 2017.

The user has requested enhancement of the downloaded file.

2017 One-Year Seismic-Hazard Forecast for the Central and Eastern United States from Induced and Natural Earthquakes

by Mark D. Petersen, Charles S. Mueller, Morgan P. Moschetti, Susan M. Hoover, Allison M. Shumway, Daniel E. McNamara, Robert A. Williams, Andrea L. Llenos, William L. Ellsworth, Andrew J. Michael, Justin L. Rubinstein, Arthur F. McGarr, and Kenneth S. Rukstales

ABSTRACT

We produce a one-year 2017 seismic-hazard forecast for the central and eastern United States from induced and natural earthquakes that updates the 2016 one-year forecast; this map is intended to provide information to the public and to facilitate the development of induced seismicity forecasting models, methods, and data. The 2017 hazard model applies the same methodology and input logic tree as the 2016 forecast, but with an updated earthquake catalog. We also evaluate the 2016 seismic-hazard forecast to improve future assessments. The 2016 forecast indicated high seismic hazard (greater than 1% probability of potentially damaging ground shaking in one year) in five focus areas: Oklahoma–Kansas, the Raton basin (Colorado/New Mexico border), north Texas, north Arkansas, and the New Madrid Seismic Zone. During 2016, several damaging induced earthquakes occurred in Oklahoma within the highest hazard region of the 2016 forecast; all of the 21 moment magnitude (**M**) ≥ 4 and 3 **M** ≥ 5 earthquakes occurred within the highest hazard area in the 2016 forecast. Outside the Oklahoma–Kansas focus area, two earthquakes with **M** ≥ 4 occurred near Trinidad, Colorado (in the Raton basin focus area), but no earthquakes with **M** ≥ 2.7 were observed in the north Texas or north Arkansas focus areas. Several observations of damaging ground-shaking levels were also recorded in the highest hazard region of Oklahoma. The 2017 forecasted seismic rates are lower in regions of induced activity due to lower rates of earthquakes in 2016 compared with 2015, which may be related to decreased wastewater injection caused by regulatory actions or by a decrease in unconventional oil and gas production. Nevertheless, the 2017 forecasted hazard is still significantly elevated in Oklahoma compared to the hazard calculated from seismicity before 2009.

INTRODUCTION

The U.S. Geological Survey (USGS) National Seismic Hazard Model Project (NSHMP) is responsible for developing seismic-hazard models for the United States that are applied in building codes, earthquake insurance, risk assessments, and other public policy applications. These long-term (i.e., 50-year) hazard assessments only take into account natural earthquakes and do not consider human-induced earthquakes (Petersen *et al.*, 2014, Petersen, Moschetti, *et al.*, 2015). This is because such seismicity typically changes rapidly over time periods of one to a few years, which is faster than the time required for approval of building codes or other public policy applications and the expected lifespan of structures. Moreover, the damage potential of such events is a relatively recent concern, spurred by the rapid increase in the rate of such activity. It is now widely acknowledged that human-induced earthquakes can cause damage, such as that which occurred in the 2011 Prague and the 2016 Cushing, Oklahoma, earthquakes (see Petersen *et al.*, 2016a, and references therein). This recognition motivates short-term assessments of seismic hazard that include humaninduced earthquakes. This assessment provides short-term damage forecasts. As we learn more about how these maps are being used, we can develop new outputs and maps that will be more useful to end users.

Most of the induced earthquake activity in the central and eastern United States (CEUS) is caused by deep wastewater disposal. Injected wastewater causes pressure changes that can weaken (unclamp) a fault and therefore bring it closer to failure. Seismicity rates in Oklahoma increased exponentially beginning in 2009 (Ellsworth, 2013), but decreased slightly (relative to 2015) in 2016. Between 1980 and 2000, Oklahoma averaged about two earthquakes greater than or equal to moment magnitude (**M**) 2.7 per year, which is the size range considered in calculating rates of future earthquakes in the one-year forecast model and in the National Seismic Hazard Models (NSHM; Petersen *et al.*, 2014). However, this number jumped to about 2500, 4000, and 2500 earthquakes in 2014, 2015, and 2016, respectively. Induced earthquakes can cause damage and therefore increase the hazard and risk across the region (see Pe-

 doi: 10.1785/0220170005

tersen, Mueller, *et al.*, 2015; Petersen *et al.*, 2016a, and references therein). During 2011, an **M** 5.7 earthquake near Prague, Oklahoma, and an **M** 5.2 earthquake near Trinidad, Colorado, caused damage to several schools and other structures (see Petersen *et al.*, 2016a, and their references section). In Oklahoma, during 2016, a 13 February **M** 5.1 earthquake near Fairview, a 3 September **M** 5.8 earthquake near Pawnee, and a 7 November **M** 5.0 earthquake near Cushing caused damaging ground shaking. These damaging events are thought to be the result of wastewater injection, and the potential for future large earthquakes causes concern to officials responsible for public safety and welfare (see Data and Resources; Keranen *et al.*, 2013; Rubinstein *et al.*, 2014; Yeck, Hayes, *et al.*, 2016).

To better estimate and communicate damage potential from induced earthquakes, the NSHMP held a workshop in 2014 with academia, industry, and government scientists to discuss how to account for the earthquake hazard and to learn about the types of products that would be helpful for public policy discussions (Petersen, Mueller, *et al.*, 2015). Attendees suggested that short-term forecasts of seismic hazard would be helpful in understanding the threat of induced seismicity and in quantifying hazard and risk for consideration in engineering applications. In 2016, a one-year seismic-hazard forecast for natural and induced earthquakes in the CEUS was developed, mostly based on 2015 earthquake rates, but also including older earthquakes (Fig. 1; Petersen *et al.*, 2016a). This forecast stated that there was a 1%–12% chance of exceeding potentially damaging ground-shaking (modified Mercalli intensity [MMI] ≥ VI) levels during 2016 in Oklahoma–Kansas, the Raton basin, north Texas, north Arkansas, and in the New Madrid Seismic Zone (NMSZ).

This article describes an updated forecast for 2017, using the same modeling framework as that of the 2016 forecast, but adding induced and natural earthquakes during 2016. In addition, we review some 2016 observations of earthquake ground motions and effects to evaluate the 2016 forecast. We discuss how government, academia, and industry are using the maps. We define five focus areas where clustered earthquakes occurred in 2016: Oklahoma–Kansas, the Raton basin (Colorado/New Mexico border), north Texas (greater Dallas/Fort Worth area), north Arkansas, and the NMSZ (Fig. 2). All of these areas except the NMSZ have experienced induced earthquake activity. Earthquake rates and estimated hazard have decreased in the five focus areas compared with the 2016 model and forecast.

COMPARISON OF 2016 FORECAST AND 2016 OBSERVATIONS

In this section, we compare the 2016 hazard forecast with the observed seismicity and ground-shaking data that were collected during that year. This analysis will help guide future earthquake forecasts and facilitate testing of the seismic-hazard forecast. We produced several types of hazard maps to better communicate the hazard. In the 2016 forecast, we converted the peak ground acceleration (PGA) and 1-s spectral acceleration (SA) hazard maps to MMI maps using the Worden *et al.* (2012) equations and averaged the maps to produce 1% in one-year probability of exceedance maps. For producing chance of damage maps, we assume that the threshold of damage is MMI VI, characterized by cracking of plaster and weak masonry. This map is developed using the hazard curves to determine the annual frequency of exceedance for $0.12g$ PGA or $0.1g$ SA at 1 s (for National Earthquake Hazard Reduction Program—site class D, Petersen *et al.*, 2016a, b).

One important observation in assessing the past forecast and producing a new forecast is that fewer declustered earthquakes occurred in 2016 than in 2015 (Fig. 2). This may be due to decreased wastewater injection, caused by lower oil prices (Murray, 2016) or by regulatory actions (see Data and Resources). The 2016 earthquake counts are lower than those in the previous year. The rate of natural earthquakes near the NMSZ is also lower, which probably has nothing to do with wastewater injection. Some of this decrease may be related to network and processing changes, but may also be related to natural variability in the seismicity rates.

We use the number of **M** ≥ 2.7 events for forecasting the rate of future earthquakes and **M** ≥ 4.7 for forecasting the ground-shaking levels. The ground-shaking calculation was lowered to **M** ≥ 4.0 in a sensitivity study by Petersen *et al.* (2016b) because lower magnitude earthquakes have caused damaging ground shaking. We use the **M** ≥ 4.7 threshold to conform with the 2016 model. During 2016, three of the five focus areas experienced earthquakes with **M** ≥ 2.7. The Oklahoma–Kansas focus area experienced about 2500 earthquakes (162 independent events), the Raton basin had 6 earthquakes (5 independent events), and the NMSZ had 24 earthquakes (20 independent events) (Fig. 3). North Arkansas and north Texas did not experience any earthquakes of this size during 2016. Even though the rates of earthquakes were lower during 2016, the seismic moment rate was higher based on the three **M** ≥ 5 earthquakes that occurred in Oklahoma (Fig. 4).

Oklahoma experienced 21 earthquakes with **M** ≥ 4.0, and the Raton basin experienced 2 such earthquakes during 2016. Only Oklahoma recorded earthquakes with **M** ≥ 4.7; there were four earthquakes, with one of these considered a dependent event (Fig. 5a). The four largest earthquakes in Oklahoma during 2016 were 13 February **M** 5.1 near Fairview and a 7 January **M** 4.8 foreshock (Yeck, Hayes, *et al.*, 2016), 3 September **M** 5.8 near Pawnee (the largest earthquake ever recorded in Oklahoma, Yeck, Weingarten, *et al.*, 2016), and 7 November **M** 5.0 near past Cushing seismicity (McNamara *et al.*, 2015).

We make an informal assessment of the validity of the 2016 model (Petersen *et al.*, 2016a, b) using the predicted shaking areas for the **M** ≥ 4 earthquakes, ShakeMap instrumental and extrapolated ground-shaking levels, "Did You Feel It?" (DYFI) responses, and the seismic stations that recorded potentially damaging strong motions. Records from these largest earthquakes indicate that MMI ≥ VI or PGA ≥ $0.12g$ were felt throughout central Oklahoma and southern Kansas in 2016. Figure 5 shows the locations of the largest earthquakes and associated data, which can be used to evalu-

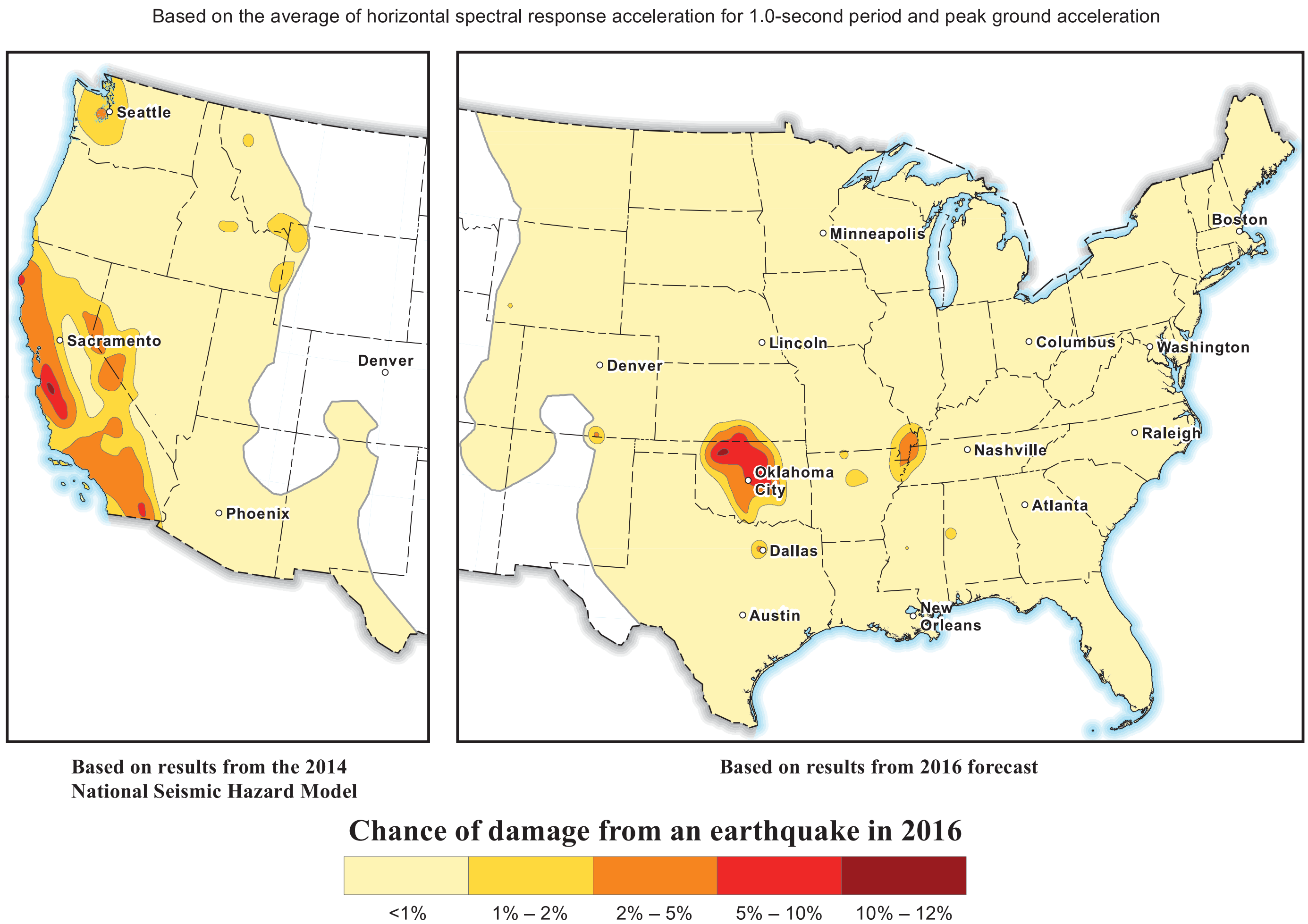

▲ **Figure 1.** (Right) 2016 one-year forecast of the potential for damage in the central and eastern United States (Petersen *et al.*, 2016a, b), along with the (left) hazard for the western United States from the 2014 National Seismic Hazard Maps (Petersen *et al.*, 2014), shown for comparison.

ate the 2016 forecast. Each panel shows the same chance-of-damage contours from the 2016 forecast.

Figure 5a shows the locations of the 21 $\mathbf{M} \geq 4$ earthquakes in Oklahoma and modeled ground shaking (10 of these earthquakes are hidden on the figure). All of these earthquakes fall within the highest hazard area (5%–12% chance of damage). Each circle encompasses the predicted area of ground shaking $\geq 0.12g$ PGA (from table 1 of Atkinson, 2015, with an effective depth of 5 km, median ground-motion model [GMM] assuming a V_{S30} of 400 m/s using amplification factors for PGA from Seyhan and Stewart, 2014). Considering only earthquakes with $\mathbf{M} \geq 4.7$, the modeled area with PGA $\geq 0.12g$ is 5.5% of the total high-shaking area within the 5%–12% chance-of-damage contour (31,700 km^2). If we consider the uncertainties (1 standard deviation) on the GMMs, we find that the lower bound of shaking covers 2.8% of the total high-shaking area, and we find the upper bound of shaking covers 17% of the total high-shaking area. Considering the smaller earthquakes that may also cause damage, $\mathbf{M} \geq 4.0$, the expected high-shaking area is 9.1% of the total high-shaking area within 5%–12% chance-of-damage contours. For Oklahoma, the modeled range of high-shaking areas is consistent with the 2016 forecast (assuming an ergodic assumption, Hanks *et al.*, 2012). Limitations of this approach are that we only consider median ground motions, average V_{S30}, and one GMM.

Figure 5b–d shows three additional datasets that are used to assess the model. Each of these datasets is limited in spatial coverage. Figure 5b shows the location of ShakeMap data for MMI ≥ VI or for PGA $\geq 0.12g$ (Worden *et al.*, 2010). Figure 5c shows locations of the 10 strong-motion stations that recorded ground shaking $\geq 0.12g$ PGA from any earthquake in 2016. These stations are sparse and are not uniformly distributed across the region. This figure also shows the stations that did not exceed the $0.12g$ PGA threshold. Figure 5d shows the DYFI data recorded for 2016 (Wald *et al.*, 2012). These data are aggregated over 10 km^2 grid cells. Therefore, it is difficult to see the individual reports, but these are also shown as small dark dots on the figure. A significant number of DYFI observations also fall outside of the highest contour area. Most of the outliers are related to the Pawnee earthquake. These ShakeMap station distribution and DYFI data are spread nonuniformly over a large area.

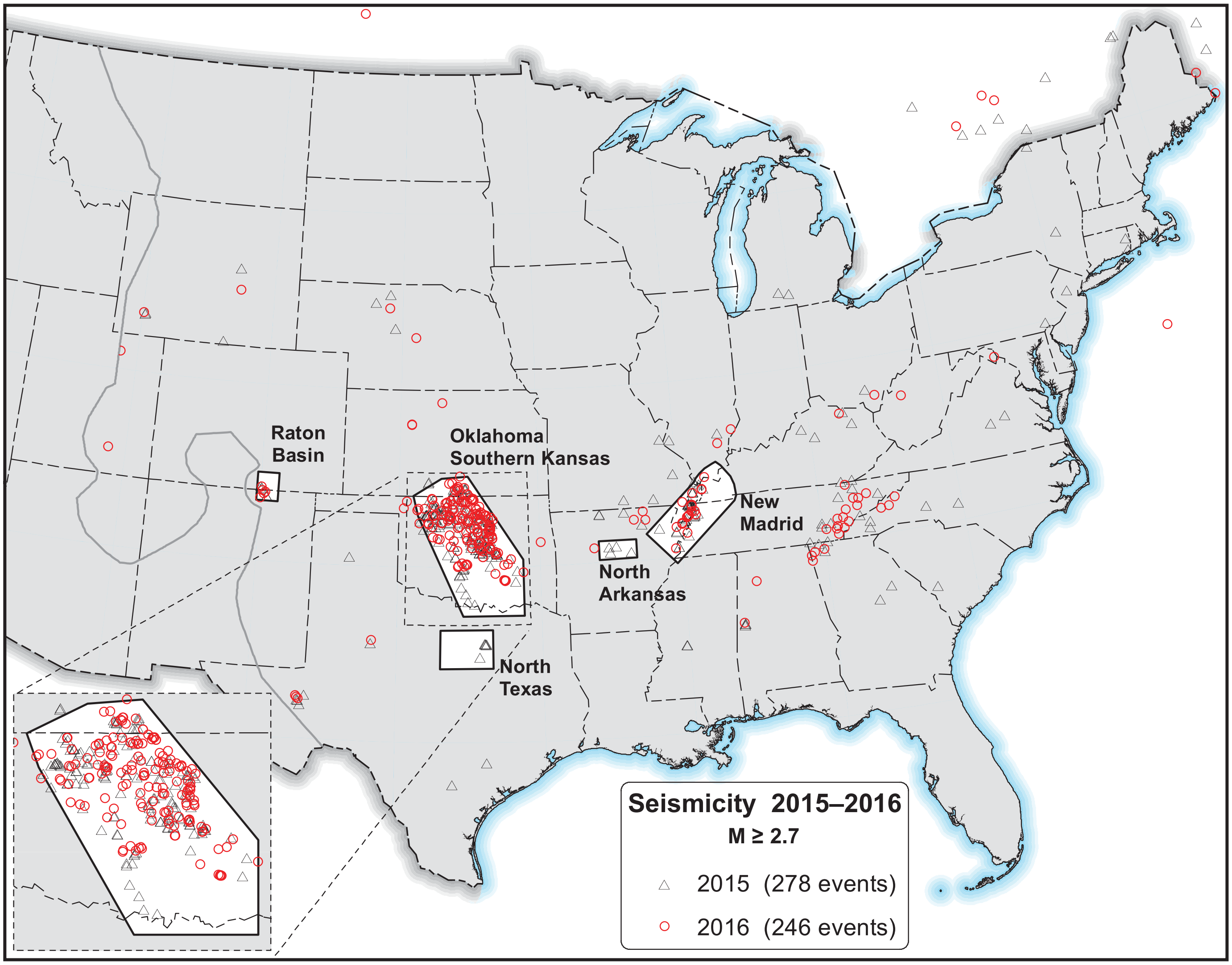

▲ **Figure 2.** Plot of 2015 (triangles) and 2016 (circles) (**M** ≥2.7) seismicity from declustered catalog. Five focus areas are Oklahoma–Kansas, Raton basin, north Texas, north Arkansas, and the New Madrid Seismic Zone.

Testing the 2016 maps is an important activity for building better models in the future, and the advantage of a short-term model is its testability. Testing allows us to explore whether our modeling was successful or unsuccessful and identify modeling parameters and assumptions that need to be refined. Several input parameters include large uncertainties (e.g., maximum magnitude, rate models, and GMMs). Figure 5 shows various types of data that allow us to test these models. All of the **M** ≥ 4 earthquakes occurred within the highest hazard contours (one-year probabilities of 5%–12%) from the 2016 forecast. The strong motion, ShakeMap, and DYFI data suggest that much of the total area enclosed by those highest probability contours may have experienced damaging ground shaking. The comparisons in Figure 5 do not constitute formal tests; however, they show that the models, which depend on past seismicity patterns, are consistent with locations of larger earthquakes and damaging ground shaking in Oklahoma in 2016. More formal tests could be devised by incorporating uncertainties in all input parameters and source models, better V_{S30} measurements and soil corrections, and alternative GMMs (both inter- and intraevent variability).

It is worth noting that the five focus areas all had lower seismicity rates in 2016 compared with those in 2015. For example, north Texas and north Arkansas did not record any **M** ≥ 2.7 earthquakes during 2016, whereas they had several earthquakes in 2015. Therefore, the 2016 observed rates were lower than the 2016 forecasted rates, which mostly depended on the 2015 catalog. The success of the 2016 forecast is dependent on earthquake rates remaining quasi stable. We recognize that the decreases in seismicity rates in north Texas and north Arkansas compared with those in 2015 make the forecasts in these areas less successful.

Figure 6 shows photographs of damage and soil liquefaction from two large 2016 earthquakes in Oklahoma. The damage (Fig. 6a) was caused by the **M** 5.0 Cushing earthquake. Unreinforced brick and stone masonry buildings

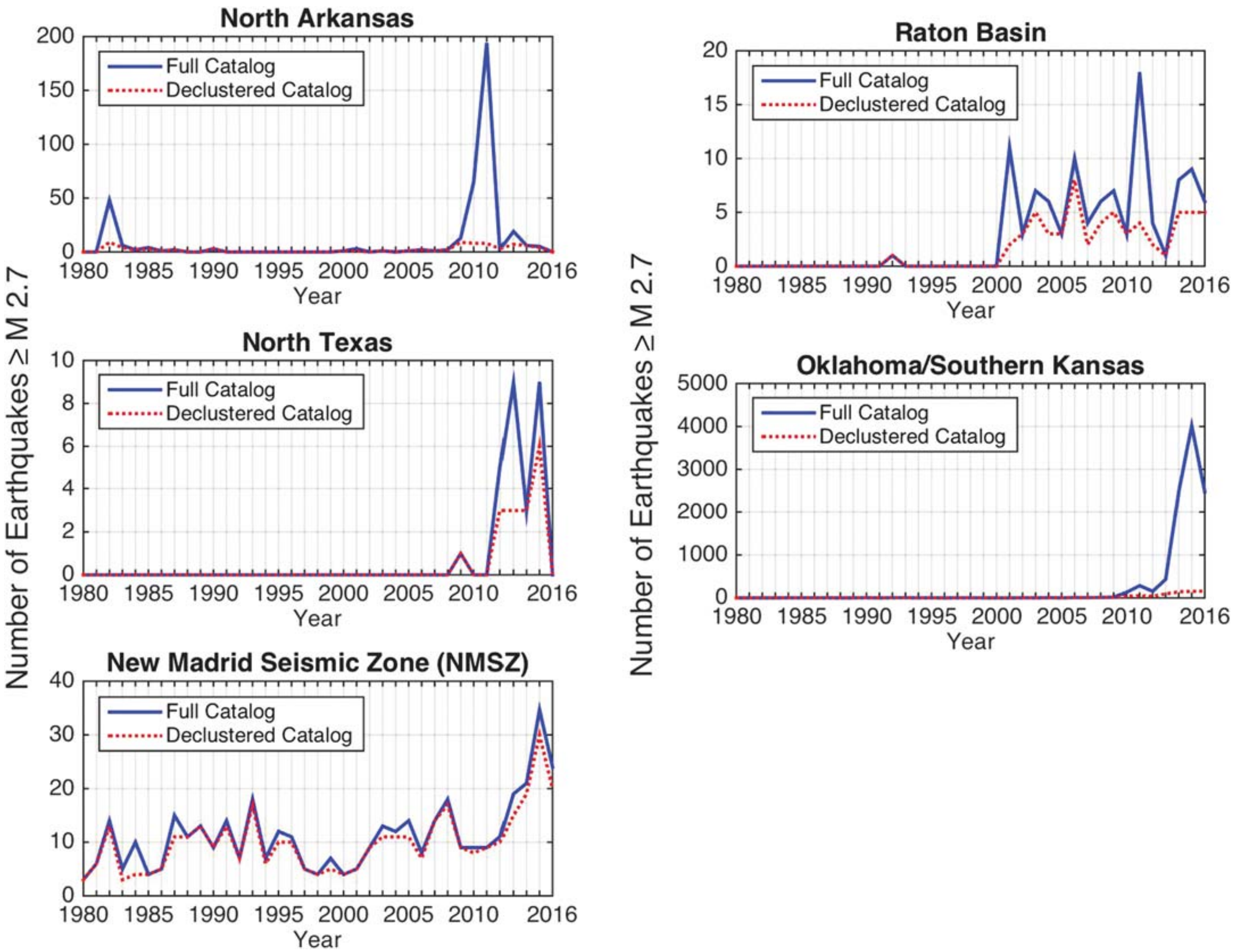

▲ **Figure 3.** The number of earthquakes with **M** ≥2.7 since 1980 in the five focus areas using the full catalog (solid lines) and the declustered catalog (dotted lines).

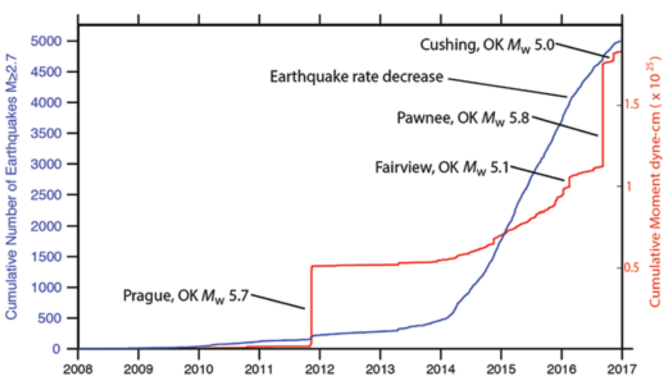

▲ **Figure 4.** Cumulative number of events (**M** ≥2.7) and cumulative moment in Oklahoma since 2008.

and facades are the most vulnerable to strong shaking. The **M** 5.8 Pawnee earthquake generated sand blows (Fig. 6b) that were observed about 8 km south of the epicenter. These figures demonstrate the types of ground shaking that are typically anticipated in the forecasted models, but stronger shaking is also possible that could cause more extensive damage.

USERS OF THE 2016 FORECAST

A number of organizations and government agencies have used the 2016 forecast in their presentations, analyses, and decision making. We do not have a complete inventory of users of this model, but we have reached out to several agencies to assess the need for such maps and to determine their usefulness. Government and academic scientists (including the Oklahoma and Kansas Geological Surveys and the Oklahoma State Insurance Department) have used the maps to discuss the hazard and risk. Risk modelers have used the input data in developing new risk assessments; they and insurance policy makers are using the maps

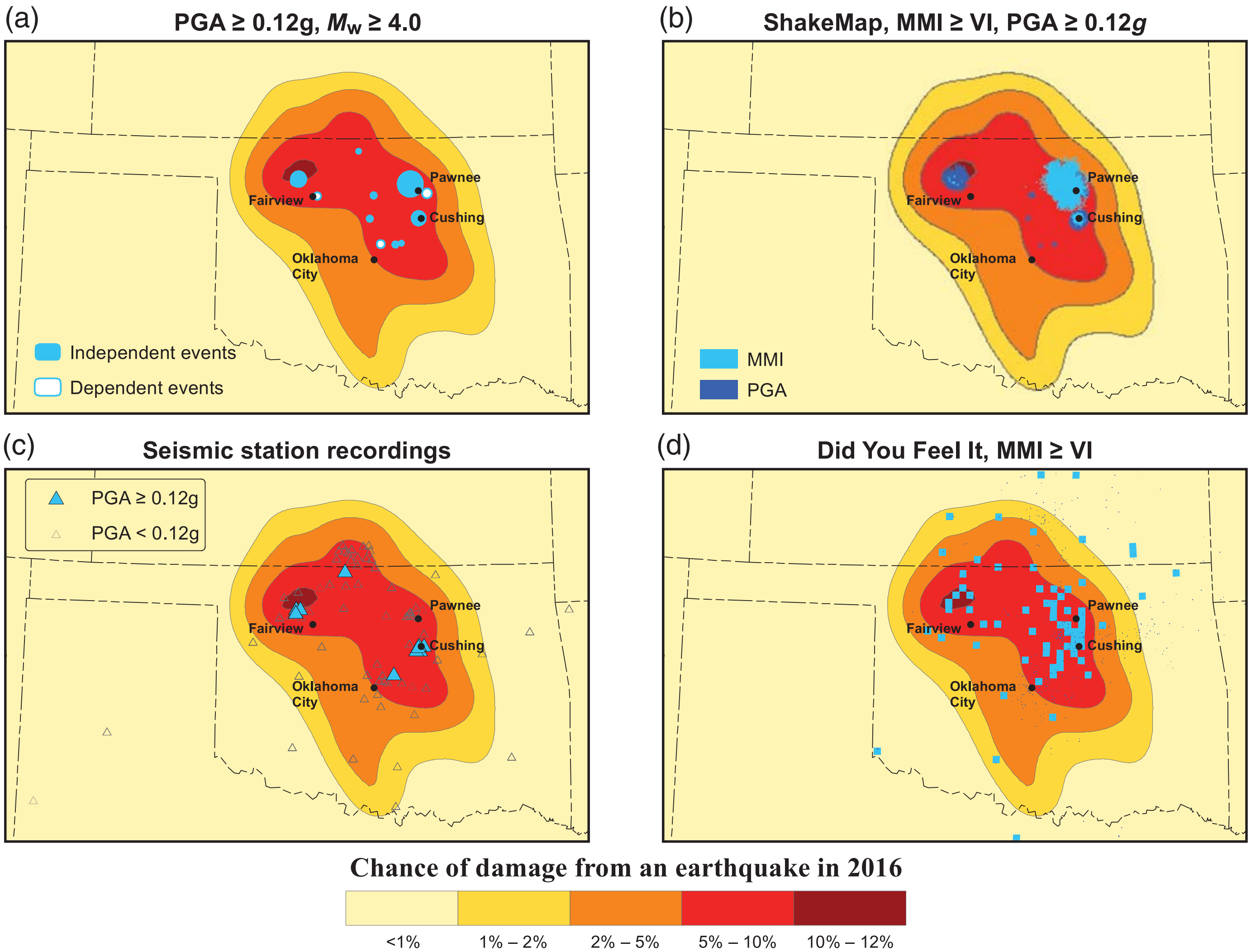

▲ **Figure 5.** Comparison of 2016 one-year forecast with potential damage data. Each panel shows the same chance-of-damage color contours from the 2016 forecast. (a) Location of **M** ≥4 earthquakes with size of the circles scaled to the distance of peak ground acceleration (PGA) ≥ 0.12*g* expected from ground-motion models, which is the threshold of modified Mercalli intensity (MMI) VI. (b) Locations of ShakeMap MMI ≥ VI or PGA ≥ 0.12*g* estimated from ShakeMap. Note that the station density is not uniform, thus it is likely that not all localities experiencing 0.12*g* are identified. (c) Locations of seismic stations that recorded PGA ≥ 0.12*g* (filled symbols) and stations that did not exceed this PGA threshold (unfilled symbols). (d) Locations of "Did You Feel It?" (DYFI) reports that exceed MMI VI from all earthquakes in 2016, shown as aggregate data (squares) and individual reports (small dots). Population density affects DYFI reporting in this figure.

to better understand the risk and potential impacts on premiums. The U.S. Army Corps of Engineers has used the information to provide guidance on updating their assessments of selected facilities in the Midcontinent. Other active users include city and county emergency managers (e.g., the Irving-Dallas Area Earthquake Working Group) and the media. More than 1000 media outlets ran stories on the maps at the time of their release, and more stories have been published during the past year.

METHODOLOGY FOR 2017 FORECAST

We use the 2016 methodology and logic trees (Petersen *et al.*, 2016a, b), but update the earthquake catalog through year 2016 and apply the long-term catalog from the 2016 study (see Data and Resources). We apply the same methodology, input parameters, and GMMs so that we can make meaningful comparisons related to the changes in seismicity rates between 2015 and 2016. We only use data derived from recent seismicity observations; we do not use data from ongoing or projected injection locations or volumes. The seismic-hazard forecast employs similar input parameters, data, models, and methods to those used for tectonic earthquakes (e.g., Petersen *et al.*, 2014; Petersen, Moschetti, *et al.*, 2015)—declustered catalogs, smoothed and gridded seismicity rates (Frankel, 1995), on-fault earthquake recurrence rates, distributions of maximum magnitude, and a suite of GMMs (Rezaeian *et al.*, 2015)—

▲ **Figure 6.** (a) Pictures of damage to buildings in Cushing, Oklahoma, from the 6 November 2016 **M** 5.0 earthquake. Unreinforced brick and stone masonry buildings and facades are vulnerable to strong shaking. (b) Sand blows were generated by the 3 September 2016 **M** 5.8 earthquake near Pawnee, Oklahoma. Liquefaction features formed near Black Bear Creek about 8 km south of the epicenter.

to compute mean rates of exceedance for a set of ground motions. We apply the standard probabilistic seismic-hazard analysis methodology (Cornell, 1968) requiring a catalog of independent earthquakes, which we obtain through declustering the catalog. We performed a sensitivity study on the influence on hazard from applying a declustered or full catalog that we presented in Petersen, Mueller, *et al.* (2015). This declustering methodology causes hazard in some places to increase and other places to decrease because the full catalog is characterized by a steeper *b*-value. For this analysis, we apply declustering as in the 2016 forecast so that we can compare the effects of the different catalogs. Future models may reconsider this declustering methodology.

The short-term seismic-hazard forecast also incorporates information specific to induced earthquakes, including modified smoothing distances and catalog durations (Moschetti *et al.*, 2016), maximum magnitudes (e.g., McGarr, 2014), and GMMs applicable to the shallower depths of induced earthquakes (e.g., Atkinson, 2015). We consider the Atkinson (2015) standard model (table 1 of Atkinson, 2015) for 2 and 5 km depths of rupture. We also apply the eight CEUS GMMs from the 2014 NSHM (Petersen *et al.*, 2014). Ground shaking is converted to MMI using the Worden *et al.* (2012) relations for PGA and 1-s SA.

We recognize that consideration of alternative input parameters and models (maximum and minimum magnitude, ground motions, rate parameters and declustering), new industrial data, and alternative rate models will improve the forecast. Over the past year, several working groups have been conducting scientific research on topics applicable to these induced seismicity models. The resulting science will be considered in future updates of the induced seismicity forecast.

2017 FORECAST RESULTS

Maps showing probabilistic ground motions for 2017 with 1% probability of exceedance in 1 year for PGA and 1-s SA are shown in Figures 7a and 7b, respectively. Although the hazard has decreased compared with that in the 2016 forecast, the maps indicate continuing high hazard in the Oklahoma–Kansas, Raton basin, and NMSZ focus areas. The hazard levels in Oklahoma are significantly higher than those in the hazard models applied in building codes that only incorporate natural earthquakes.

From the PGA and 1-s SA maps, we produce MMI maps to better delineate where the potentially damaging ground shaking is anticipated. Both PGA and 1-s SA are used in calculating MMI to give a more robust estimate of the intensity (Worden *et al.*, 2012). In Figure 8a, we present a 1% probability of exceedance in the one-year map for MMI that is amplified by soils as in Petersen *et al.* (2016a). This map contains similar patterns to the PGA and 1-s SA upon which the MMI map is based. The MMI ≥ VI maps represent the threshold of damage, and this intensity level is used to produce a chance-of-damage map for 2017 (Fig. 8b). The chance-of-damage map highlights mostly Oklahoma earthquakes because they have been so numerous over the past year. Figure 9 shows a large-scale chance of damage map showing the 2016 and 2017 one-year forecasts. Other products, such as the seismicity catalogs used in this study, hazard curves, and additional hazard maps, are available at ScienceBase (see Data and Resources).

The seismic-hazard forecast for 2017 is lower than that in the 2016 forecast, because seismicity rates were lower in 2016 compared with those in 2015 (Fig. 9). All five focus areas experienced fewer earthquakes in 2016 than in 2015 (Fig. 2). In particular, in Oklahoma during the last six months of 2016, the rates were significantly lower than the rates observed during the previous two years. This observation, along with the research by Llenos *et al.* (2015), indicates that it may be helpful to also include a 6-month-based forecast.

CONCLUSIONS

This report documents a one-year 2017 forecast for seismic hazard in the CEUS from induced and natural earthquakes that may be useful for the public and policy officials, and may have some engineering applications. The model was developed for one year, and we do not recommend applying the results for very low rates of exceedance in which the model is not as well constrained as shorter rates of exceedance. The 2017 forecasted hazard is still high in Oklahoma but is lower compared with the 2016 model in the five focus areas analyzed in this article. Earthquake rate decreases during the past year may be related to the lower price of oil (Murray, 2016) or regulatory actions (Langenbruch and Zoback, 2016; Yeck, Weingarten, *et al.*, 2016; see Data and Resources).

The locations of $\mathbf{M} \geq 4$ earthquakes, ShakeMap data, DYFI data, and strong-motion observations and measurements indicate (qualitatively) that the 2016 forecast performed well in Oklahoma. However, in other locations, the rates were lower than those predicted in our 2016 forecast. Our forecast assumes that seismicity will be stationary over the year. When seismicity rates change significantly over a year, which occurred in 2016 in north Texas and north Arkansas, the forecast is not as successful. Additional information on industrial processes in these areas will help us refine these forecasts in the future. Models would be improved with this information as well as new data models and methods that better describe future earthquake sources and ground-shaking levels.

Forecasting induced seismic hazard is difficult because of the high uncertainties in the input parameters and the uncertainty due to rapid fluctuations in industrial activity, which is not included in the current model. Nevertheless, our results indicate that the 2017 forecasted hazard is considerably higher than the hazard calculated in the 2014 NSHM (Petersen *et al.*, 2014; Petersen, Moschetti, *et al.*, 2015). Our results confirm the statement by Langenbruch and Zoback (2016) that the possibility of damaging earthquakes during 2017 cannot be discounted.

For Oklahoma and southern Kansas, these new results show that about 3 million people live with continuing increased potential for damaging shaking from induced seismicity, and the

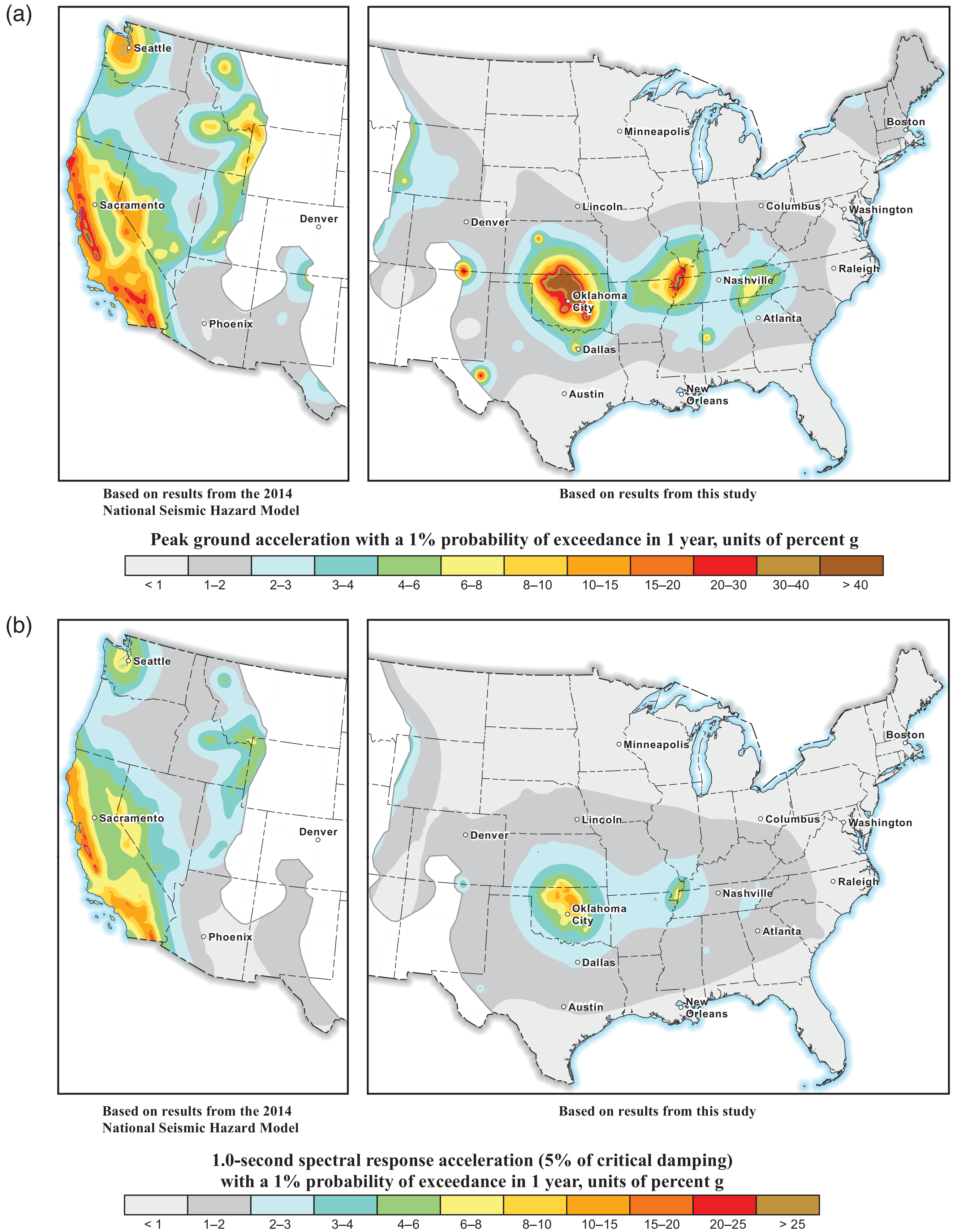

▲ **Figure 7.** (a) PGA and (b) 1 s spectral acceleration (SA) for 1% probability of exceedance in 2017. Hazard for the western United States from the 2014 National Seismic Hazard Maps (Petersen *et al.*, 2014) is shown for comparison.

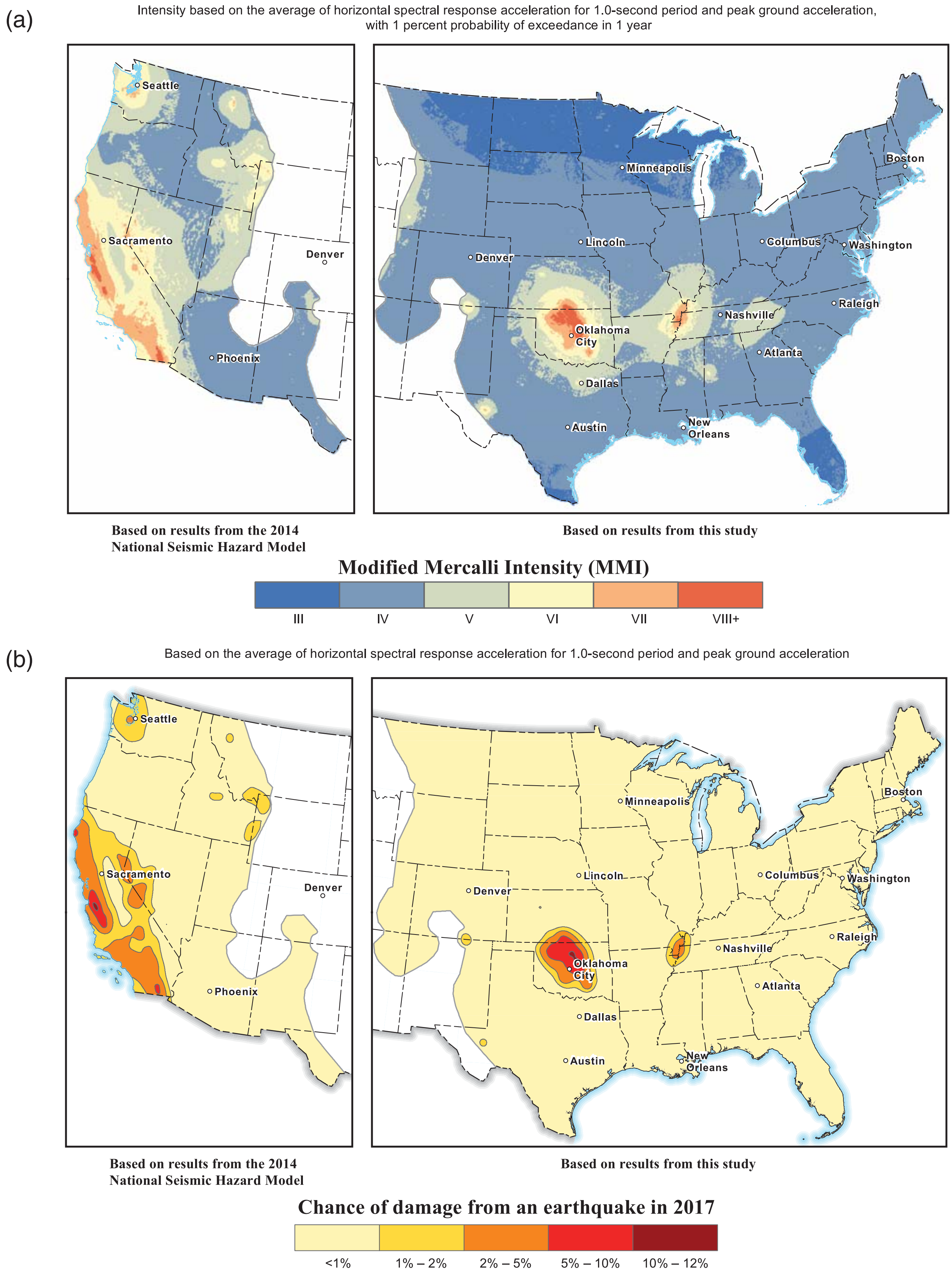

▲ **Figure 8.** (a) MMI for 1% probability of exceedance in 1 year. (b) Chance of damage from an earthquake in 2017. Hazard for the western United States from the 2014 National Seismic Hazard Maps (Petersen *et al.*, 2014) is shown for comparison.

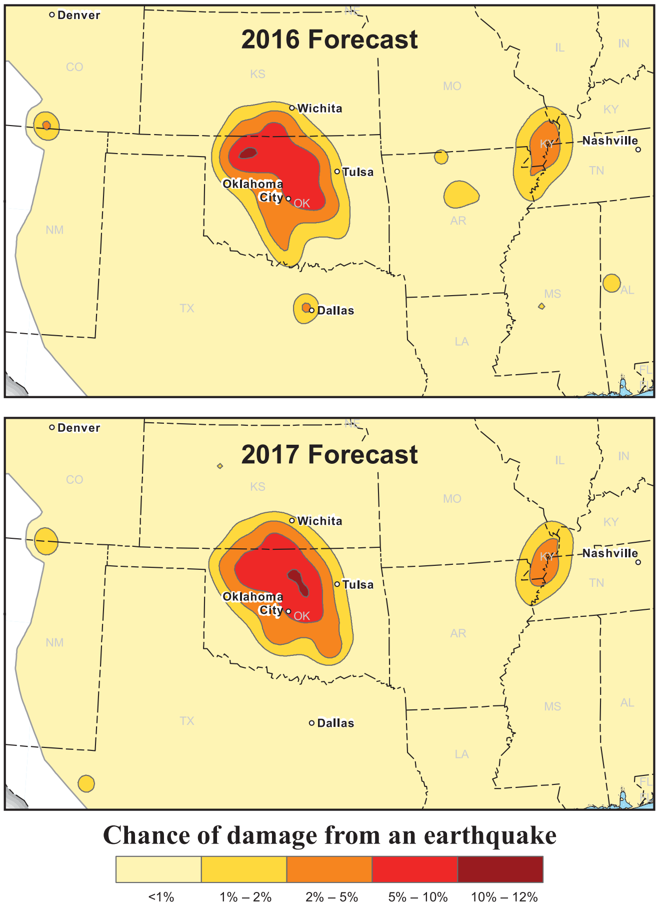

▲ **Figure 9.** Larger scale chance-of-damage maps for the 2016 and 2017 one-year forecasts for comparison.

chance of damage in the next year from induced earthquakes is still similar to that of natural earthquakes in high-hazard areas of California. Significant damage in 2016 occurred to unreinforced masonry buildings in Pawnee and Cushing, Oklahoma. The threat of future damage, particularly to older unreinforced brick and stone structures, remains.

Although the focus of this article is on updating the 2016 one-year forecast for 2017 and assessing the performance of the 2016 one-year forecast model, we also acknowledge that the hazard assessment methodology can and will advance with additional research. Development of new induced seismicity GMMs, analysis of catalog statistics, assessment of differences in induced and natural earthquake sources, estimation of potential maximum magnitude induced earthquakes, consideration of alternative seismic rate models that are constrained by physics, and tests of models that identify parameters are all areas where research could improve the methodology. In addition, improving our estimation of input parameter uncertainties and including additional industry information would enhance the model. We welcome the support of other government agencies, academia, and industry in improving the data, models, and methods applied in these models.

DATA AND RESOURCES

An example of regulatory actions and policy officials responding to earthquakes caused by induced seismicity can be found at http://www.occeweb.com/News/2016/11-23-16EARTHQUAKE ACTION SUMMARY.pdf (last accessed February 2017). The seismicity catalogs for the 2017 central and eastern United States (CEUS) short-term seismic-hazard model are located at doi: 10.5066/F7KP80B9. The datasets for this study, including the declustered seismicity catalogs, can be found at doi: 10.5066/F7RV0KWR.

ACKNOWLEDGMENTS

We thank Paul Earle, Bruce Presgrave, the National Earthquake Information Center (NEIC) team for expediting the release of the 2016 ComCat catalog early in 2017, and the regional network operators who have contributed to the seismic data. We also thank members of the National Seismic Hazard And Risk Assessment Steering Committee: John Anderson (chair), Norm Abrahamson, Kenneth Campbell, Martin Chapman, Michael Hamburger, William Lettis, Nilesh Shome, Ray Weldon, and Chris Wills, who reviewed the documentation, data, methods, and models, and provided important feedback that helped us to improve the quality of this article. In addition, Will Yeck, Michael Blanpied, Gail Atkinson, Cliff Frohlich, Jill McCarthy, and Tom Hanks provided important comments and ideas that were incorporated in the report. Finally, we thank the U.S. Geological Survey Earthquake Hazard Program for funding the development of the maps.

REFERENCES

Atkinson, G. M. (2015). Ground-motion prediction equation for small-to-moderate events at short hypocentral distances, with application to induced-seismicity hazards, *Bull. Seismol. Soc. Am* **105,** no. 2A, 981–992, doi: 10.1785/0120140142.

Cornell, C. A. (1968). Engineering seismic risk analysis, *Bull. Seismol. Soc. Am* **58,** 1583–1606.

Ellsworth, W. L. (2013). Injection-induced earthquakes, *Science* **341,** no. 6142, doi: 10.1126/science.1225942.

Frankel, A. (1995). Mapping seismic hazard in the central and eastern United States, *Seismol. Res. Lett.* **66,** no. 4, 8–21, doi: 10.1785/gssrl.66.4.8.

Hanks, T. C., G. C. Beroza, and S. Toda (2012). Have recent earthquakes exposed flaws in or misunderstandings of probabilistic seismic hazard analysis, *Seismol. Res. Lett.* **83,** 759–764, doi: 10.1785/0220120043.

Keranen, K. M., H. M. Savage, G. A. Abers, and E. S. Cochran (2013). Potentially induced earthquakes in Oklahoma, USA: Links between wastewater injection and the 2011 M_w 5.7 earthquake sequence, *Geology* **41,** no. 6, 699–702, doi: 10.1130/G34045.1.

Langenbruch, C., and M. D. Zoback (2016). How will induced seismicity in Oklahoma respond to decreased saltwater injection rates? *Sci. Adv.* **2,** no. 11, 10, doi: 10.1126/sciadv.1601542.

Llenos, A. L., W. L. Ellsworth, and A. L. Michael (2015). Earthquake rate models for evolving induced seismicity hazard in the central and eastern US, presented at the *American Geophysical Union, Fall Meeting*, San Francisco, California, 14–18 December 2015.

McGarr, A. (2014). Maximum magnitude earthquakes induced by fluid injection, *J. Geophys. Res.* **119,** no. 2, 1008–1019, doi: 10.1002/2013JB010597.

McNamara, D. E., G. P. Hayes, H. M. Benz, R. A. Williams, N. D. McMahon, R. C. Aster, A. Holland, T. Sickbert, R. Herrmann, R. Briggs, *et al.* (2015). Reactivated faulting near Cushing Oklahoma: Increased potential for a triggered earthquake in an area of United States strategic infrastructure, *Geophys. Res. Lett.* **42,** no. 20, 8328–8332, doi: 10.1002/2015GL064669.

Moschetti, M. P., S. M. Hoover, and C. S. Mueller (2016). Likelihood testing of seismicity-based rate forecasts of induced earthquakes in Oklahoma and Kansas, *Geophys. Res. Lett.* **43,** 4913–4921, doi: 10.1002/2016GL068948.

Murray, K. E. (2016). Seismic moment versus water: A study of market forces and regulatory actions, Paper No. 95-11, presented at the *GSA Annual Meeting*, Denver, Colorado, 25–28 September 2016, doi: 10.1130/abs/2016AM-286149.

Petersen, M. D., M. P. Moschetti, P. M. Powers, C. S. Mueller, K. M. Haller, A. D. Frankel, Y. Zeng, S. Rezaeian, S. C. Harmsen, O. S. Boyd, *et al.* (2014). Documentation for the 2014 update of the United States National Seismic Hazard Maps, *U.S. Geol. Surv. Open-File Rept. 2014-1091*, 243 pp., doi: 10.3133/ofr20141091.

Petersen, M. D., M. P. Moschetti, P. M. Powers, C. S. Mueller, K. M. Haller, A. D. Frankel, Y. Zeng, S. Rezaeian, S. C. Harmsen, O. S. Boyd, *et al.* (2015). The 2014 United States National Seismic Hazard Model, *Earthq. Spectra* **31,** no. S1, S1–S30, doi: 10.1193/120814EQS210M.

Petersen, M. D., C. S. Mueller, M. P. Moschetti, S. M. Hoover, A. L. Llenos, W. L. Ellsworth, A. J. Michael, J. L. Rubinstein, A. F. McGarr, and K. S. Rukstales (2016a). 2016 one-year seismic hazard forecast for the central and eastern United States from induced and natural earthquakes, *U.S. Geol. Surv. Open-File Rept. 2016-1035*, 52 pp., doi: 10.3133/ofr20161035.

Petersen, M. D., C. S. Mueller, M. P. Moschetti, S. M. Hoover, A. L. Llenos, W. L. Ellsworth, A. J. Michael, J. L. Rubinstein, A. F. McGarr, and K. S. Rukstales (2016b). Seismic-hazard forecast for 2016 including induced and natural earthquakes in the central and eastern United States, *Seismol. Res. Lett.* **87,** no. 6, 1327–1341, doi: 10.1785/0220160072.

Petersen, M. D., C. S. Mueller, M. P. Moschetti, S. M. Hoover, J. L. Rubinstein, A. L. Llenos, A. J. Michael, W. L. Ellsworth, A. F. McGarr, A. A. Holland, *et al.* (2015). Incorporating induced seismicity in the 2014 United States national seismic hazard model—Results of 2014 workshop and sensitivity studies, *U.S. Geol. Surv. Open-File Rept. 2015-1070*, 69 pp., doi: 10.3133/ofr20151070.

Rezaeian, S., M. D. Petersen, and M. P. Moschetti (2015). Ground motion models used in the 2014 US national seismic hazard maps, *Earthq. Spectra* **31,** no. S1, S59–S84, doi: 10.1193/111714EQS194M.

Rubinstein, J. L., W. L. Ellsworth, A. McGarr, and H. M. Benz (2014). The 2001-present induced earthquake sequence in the Raton basin of northern New Mexico and southern Colorado, *Bull. Seismol. Soc. Am.* **104,** no. 5, 2162–2181, doi: 10.1785/0120140009.

Seyhan, E., and J. P. Stewart (2014). Semi-empirical nonlinear site amplification from NGA-West2 data and simulations, *Earthq. Spectra* **30,** no. 3, 1241–1256, doi: 10.1193/063013EQS181M.

Wald, D. J., V. Quitoriano, C. B. Worden, M. Hopper, and J. W. Dewey (2012). USGS "Did You Feel It?" internet-based macroseismic intensity maps, *Ann. Geophys.* **54,** no. 6, 688–707, doi: 10.4401/ag-5354.

Worden, C. B., M. C. Gerstenberger, D. A. Rhoades, and D. J. Wald (2012). Probabilistic relationships between ground-motion parameters and modified Mercalli intensity in California, *Bull. Seismol. Soc. Am.* **102,** no. 1, 204–221, doi: 10.1785/0120110156.

Worden, C. B., D. J. Wald, K. Lin, D. Garcia, and G. Cua (2010). A revised ground- motion and intensity interpolation scheme for ShakeMap, *Bull. Seismol. Soc. Am.* **100,** no. 6, 3083–3096, doi: 10.1785/0120100101.

Yeck, W. L., G. P. Hayes, D. E. McNamara, J. L. Rubinstein, W. Barnhart, P. S. Earle, and H. M. Benz (2016). Oklahoma experiences largest earthquake during ongoing regional wastewater injection hazard mitigation efforts, *Geophys. Res. Lett.*, doi: 10.1002/2016GL071685.

Yeck, W. L., M. Weingarten, H. M. Benz, D. E. McNamara, E. Bergman, R. B. Herrmann, J. Rubinstein, and P. S. Earle (2016). Far-field pressurization likely caused one of the largest injection induced earthquakes by reactivating a large pre-existing basement fault structure, *Geophys. Res. Lett.* **43,** no. 19, 10,198–10,207, doi: 10.1002/2016GL070861.

Mark D. Petersen
Charles S. Mueller
Morgan P. Moschetti
Susan M. Hoover
Allison M. Shumway
Daniel E. McNamara
Robert A. Williams
Kenneth S. Rukstales
U.S. Geological Survey
MS 966, Box 25046
Denver, Colorado 80225 U.S.A.
mpetersen@usgs.gov

Andrea L. Llenos
Andrew J. Michael
Justin L. Rubinstein
Arthur F. McGarr
U.S. Geological Survey
345 Middlefield Road, MS 977
Menlo Park, California 94025 U.S.A.

William L. Ellsworth
Department of Geophysics
Stanford University
397 Panama Mall
Mitchell Building Room 373B
Stanford, California 94305 U.S.A.

Published Online 1 March 2017

View publication stats